The EMBO Journal (2012) 31, 805–816 | © 2012 European Molecular Biology Organization | All Rights Reserved 0261-4189/12
www.embojournal.org

THE EMBO JOURNAL

Metaplasticity gated through differential regulation of GluN2A versus GluN2B receptors by Src family kinases

Kai Yang[1,6], Catherine Trepanier[2,6], Bikram Sidhu[1,6], Yu-Feng Xie[3], Hongbin Li[1], Gang Lei[3], Michael W Salter[4], Beverley A Orser[1], Takanobu Nakazawa[5], Tadashi Yamamoto[5], Michael F Jackson[3,*] and John F MacDonald[1,2,3]

[1]Department of Physiology, University of Toronto, Toronto, Ontario, Canada, [2]Department of Pharmacology, University of Toronto, Toronto, Ontario, Canada, [3]Molecular Brain Research Group, Robarts Research Institute and the Department of Physiology and Pharmacology, The University of Western Ontario, London, Ontario, Canada, [4]Program in Neuroscience and Mental Health, Hospital for Sick Children, Toronto, Ontario, Canada and [5]Division of Oncology, Institute of Medical Science, University of Tokyo, Tokyo, Japan

Metaplasticity is a higher form of synaptic plasticity that is essential for learning and memory, but its molecular mechanisms remain poorly understood. Here, we report that metaplasticity of transmission at CA1 synapses in the hippocampus is mediated by Src family kinase regulation of NMDA receptors (NMDARs). We found that stimulation of G-protein-coupled receptors (GPCRs) regulated the absolute contribution of GluN2A-versus GluN2B-containing NMDARs in CA1 neurons: pituitary adenylate cyclase activating peptide 1 receptors (PAC1Rs) selectively recruited Src kinase, phosphorylated GluN2ARs, and enhanced their functional contribution; dopamine 1 receptors (D1Rs) selectively stimulated Fyn kinase, phosphorylated GluN2BRs, and enhanced these currents. Surprisingly, PAC1R lowered the threshold for long-term potentiation while long-term depression was enhanced by D1R. We conclude that metaplasticity is gated by the activity of GPCRs, which selectively target subtypes of NMDARs via Src kinases.

The EMBO Journal (2012) **31,** 805–816. doi:10.1038/emboj.2011.453; Published online 20 December 2011
Subject Categories: signal transduction; neuroscience
Keywords: NMDA receptors; Src kinases; synaptic plasticity

Introduction

Various forms of synaptic plasticity at CA1 synapses are dependent upon activation of postsynaptic NMDA receptors (NMDARs; Collingridge and Bliss, 1995; Abraham, 2008), providing mechanisms underlying important aspects of hippocampal learning and memory (Whitlock *et al*, 2006; Howland and Wang, 2008). Two major subtypes of NMDARs are located at these synapses; they are heterotetramers composed predominantly of GluN1a in combination with either GluN2A (GluN2ARs) or GluN2B (GluN2BRs) subunits. The requirement for receptor subtypes at these synapses is poorly understood. Each subtype is calcium permeable but differences in their gating kinetics and topographical location in the cell result in distinct temporal and spatial intracellular calcium signals (Kohr, 2006; Berberich *et al*, 2007). For example, GluN2ARs activate and deactivate more rapidly than do GluN2BRs, allowing for a substantive but transient entry of Ca^{2+} via GluN2ARs versus a much slower, but in total, much larger total charge transfer for Ca^{2+} via GluNR2BRs (Vicini *et al*, 1998). Therefore, each receptor subtype might dramatically differ in its contribution to Ca^{2+}-dependent signalling and synaptic plasticity (Cull-Candy and Leszkiewicz, 2004). The relative contributions of NMDAR subtypes to the direction of synaptic plasticity (potentiation versus depression) have been highly controversial, ranging from distinct roles for GluN2ARs in long-term potentiation (LTP) versus GluN2BRs in long-term depression (LTD; Liu *et al*, 2004; Fox *et al*, 2006; Brigman *et al*, 2010), to the assertion that it is the ratio of GluN2AR/GluN2BR, which determines direction (Cho *et al*, 2009). Just as significantly, whether signal transduction cascades can alter the relative contribution of each receptor subtype, and thus dynamically alter the direction of synaptic plasticity has not previously been explored.

Protein tyrosine phosphorylation provides a powerful means of regulating NMDAR function in the CNS (Salter and Kalia, 2004; Chen and Roche, 2007). The phosphorylation status of NMDAR subunits is set by the concerted and opposing activity of specific kinases and phosphatases, and may be dynamically altered by prior neuronal activity or through the engagement of specific intracellular signalling cascades. In this respect, Src family kinases play an essential role in initiating activity-dependent synaptic plasticity without themselves changing synaptic efficacy (Lu *et al*, 1998; Ali and Salter, 2001; Huang *et al*, 2001; Salter and Kalia, 2004; Xu *et al*, 2008). At CA1 synapses, the activity of the tyrosine kinases Src and Fyn is required for the induction of LTP (Lu *et al*, 1998; Huang *et al*, 2001). However, it is unclear if and how Src and Fyn might differentially regulate the function of NMDARs in hippocampal neurons (Salter and Kalia, 2004). We hypothesized that different classes of G-protein-coupled receptors (GPCRs) (Gαq versus Gαs) activate either Src or Fyn kinase; and, that Src and Fyn selectively phosphorylate GluN2ARs or GluN2BRs, respectively. By this means each signalling pathway might selectively alter the function of each subtype of NMDARs, and as consequence, govern the direction of synaptic plasticity.

Results

GluN2A is required for Src regulation of NMDAR-mediated currents in isolated CA1 neurons

We previously showed that low concentrations of pituitary adenylate cyclase activating peptide 38 (PACAP38) potentiated

*Corresponding author. Robarts Research Institute, 100 Perth Drive, London, Ontario, Canada N6A 5K8. Tel.: +519 931 5777/ext. 24230; Fax: +519 931 5721; E-mail: mjackson@robarts.ca
[6]Co-first authors

Received: 16 February 2011; accepted: 11 November 2011; published online: 20 December 2011

NMDA-induced currents (via the PAC_1R) in isolated CA1 pyramidal neurons, and this effect was prevented by co-application of the Src interfering peptide Src(40–58) (Macdonald *et al*, 2005). This peptide does not inhibit the enzymatic activity of Src, but rather interferes with the binding of Src to the scaffolding protein, NADH dehydrogenase subunit 2, thus preventing Src from orienting to a subcellular compartment where it can phosphorylate NMDARs (Gingrich *et al*, 2004).

For whole-cell recordings from isolated CA1 neurons from rats and mice, NMDA (50 μM NMDA and 500 nM glycine) applications of 3 s duration were repeated at a frequency of 1 per minute using one barrel of a rapid perfusion system while a second barrel was used to apply control bathing solution. Tests on cells from transgenic mice were always matched with appropriate controls from wild-type mice. Recovery from GluN2R desensitization was complete between applications. Recombinant kinases, interfering peptides (e.g., Src(40–58) and PKI_{5-24}) were included in the patch recording pipette. In some experiments, where indicated, we doubled the concentration of NMDA (100 μM) and glycine (1 μM) in order to achieve responses of comparable amplitude to those of controls. Receptor agonists such as PACAP38 and SKF81297 were applied together with NMDA in the first barrel as well as the control barrel, for a period of 5 min as indicated in the figures (shaded regions). In contrast, antagonists were applied continuously in both the control barrel and the NMDA-containing barrel of the perfusion system throughout the entire duration of the recordings.

We initially examined the effects of intracellular applications of recombinant Src (30 U/ml, patch electrode) upon peak NMDA current (50 μM NMDA and 500 nM glycine). The Src-induced potentiation was insensitive to the highly selective GluN2BR inhibitor, Ro 25-6981 (500 nM) (Fischer *et al*, 1997; Malherbe *et al*, 2003), but was strongly inhibited by the GluN2AR competitive antagonist, NVP-AAM077 (50 nM) (Neyton and Paoletti, 2006; Bartlett *et al*, 2007; Paoletti and Neyton, 2007; Figure 1A and B). Given the relatively limited selectivity of NVP-AAM077, we further tested Zn^{2+} at a concentration (300 nM) shown to preferentially block GluN2ARs versus GluN2BRs in the hippocampus (Neyton and Paoletti, 2006; Paoletti and Neyton, 2007; Nozaki *et al*, 2011). Zinc blocked the potentiation of NMDA-evoked currents by Src (Figure 1B). Furthermore, in CA1 neurons from wild-type mice Src enhanced peak currents but these effects were absent (Figure 1B) in cells from $GluN2A^{-/-}$ knockout mice (Ito *et al*, 1997). We then used a low concentration of the PAC_1R agonist, PACAP38 (1 nM, 5 min, perfusion barrels) (Macdonald *et al*, 2005) to activate endogenous Src in these neurons (Macdonald *et al*, 2005). The PAC_1Rs effects were not blocked by Ro 25-6981 (500 nM) or ifenprodil (3 μM) but were blocked by Zn^{2+} (300 nM) and NVP-AAM077 (50 nM). Furthermore, its effects were absent in cells from $GluN2A^{-/-}$ mice (Figure 1C and D).

GluN2B and not GluN2A is required for Fyn regulation of NMDAR-mediated currents in isolated CA1 neurons

Fyn kinase has been implicated many times in the regulation of NMDARs (Salter and Kalia, 2004). However, whether such regulation is GluN2 subunit dependent has not been shown. We therefore compared the effects of recombinant Fyn kinase (1 U/ml, patch electrode) on NMDAR-mediated currents with those of recombinant Src. Fyn also enhanced these currents and this effect was prevented by Ro 25-6981 (500 nM) but not by NVP-AAM077 (50 nM) (Figure 2A and B). Using an analogous approach to that used to develop Src(40–58), we synthesized a peptide corresponding to a region of the unique domain of Fyn (amino acids 39–57). We speculated that Fyn must locate to the vicinity of the receptor by binding to an unknown scaffolding protein. Fyn(39–57) (25 ng/ml), but not Src(40–58) (25 ng/ml), attenuated the effect of Fyn (Supplementary Figure S1B). Importantly, we confirmed that co-applications of Src(40–58) (25 ng/ml) prevented the enhancement of NMDA-induced currents by recombinant Src (Supplementary Figure S1A) and, conversely, showed that Fyn(39–57) did not alter the potentiation by Src kinase (Supplementary Figure S1B). These findings illustrate that this peptide can distinguish between the Src- and Fyn-dependent regulation of NMDARs. Again, it is important to note that neither peptide serves as an inhibitor of enzymatic activity (Gingrich *et al*, 2004).

GPCRs coupled to Gαs can also potentiate NMDAR currents in hippocampal neurons (MacDonald *et al*, 2007). We therefore examined the effects of stimulating the dopamine D1 receptor (D1R; Cepeda and Levine, 2006). In these recordings, we did not alter the concentrations of NMDA and glycine (50 and 0.5 μM, respectively). As a consequence, the proportionate enhancement of the contribution of the spared subtype of receptor is much greater. Application of the D1R agonist, SKF81297 (10 μM, 5 min, perfusion barrels), enhanced NMDAR currents in isolated CA1 neurons (Figure 2C). The effect of SKF81297 was blocked by the D1,5 antagonist, SCH23390 (10 μM). Block of GluN2BRs by Ro 25-6981 prevented this enhancement while block of GluN2ARs with NVP-AAM077, rather than just preventing, actually increased the proportional enhancement by D1R (Figure 2C and D). This enhancement is anticipated because blocking GluNR2ARs will result in currents generated in greater proportion by GluNR2BRs. Similar findings were observed with the GluN2AR antagonist Zn^{2+}. More convincingly, the enhancements were also proportionately larger in CA1 neurons taken from GluN2A knockout mice (Figure 2D). In addition, the potentiation by SKF81297 was prevented by the specific PKA inhibitors PKI_{5-24} (Figure 2D, applied via the patch pipette) and Rp-cAMPs (patch pipette). Similarly, applications of vasoactive intestinal peptide (VIP, 1 nM), acting through the VPAC1,2R (VIP receptors; Yang *et al*, 2009), enhanced NMDAR-mediated currents by targeting GluN2BRs (Supplementary Figure S2). Therefore, we determined if D1R and VPACR stimulations required Fyn activation rather than Src. Fyn(39–57) blocked the enhancement of NMDAR currents by each of these GPCRs (Figure 2D; Supplementary Figure S2B).

Selective phosphorylation of GluN2A and GluN2B

We also examined both the biochemical and electrophysiological actions of these GRPCRs in rat hippocampal slices. Slices were prepared as for electrophysiological recording and were similarly treated with agonists and antagonists. We demonstrated that PACAP38 treatment (1 nM for 10 min) increased Src kinase activity (increased Tyr-416 phosphorylation), but not that of Fyn (Tyr-420 phosphorylation unchanged, Figure 3A), and increased the tyrosine phosphorylation of GluN2A, but not GluN2B subunits (Figure 3B).

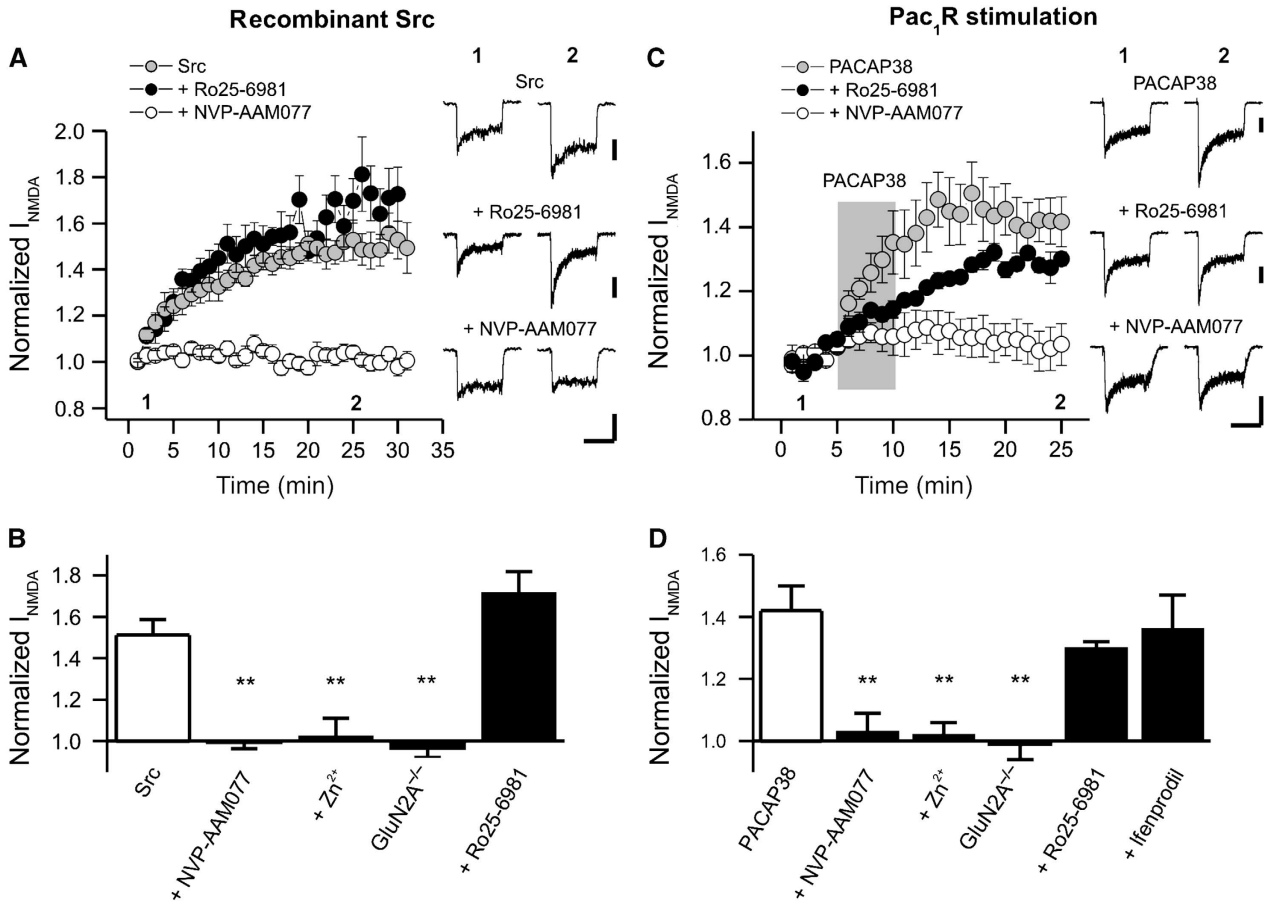

Figure 1 PAC1R-Src activation potentiates GluN2A-containing NMDAR currents in acutely isolated CA1 neurons of the rat but not in cells isolated from GluN2A$^{-/-}$ mice. (**A**) Src-mediated increase of NMDAR currents (I_{NMDA}) in hippocampal neurons (number of cells, $N=8$) is blocked by NVP-AAM077 ($N=7$) but not by Ro 25-6981 ($N=6$). Recombinant Src (30 U/ml) was applied via the patch pipette. NVP-AAM077, Zn^{2+}, and Ro25-6981 were applied to the bath and to the perfusion solutions containing NMDA/Glycine. (**B**) Src potentiation of I_{NMDA} is blocked by NVP-AAM077 ($N=7$), Zn^{2+} ($N=5$), and GluN2A deletion ($N=6$), but not by Ro25-6981 ($N=6$). Src enhanced currents in cells from wild-type mice ($N=6$, 1.7 ± 0.2 times) but not from GluN2A$^{-/-}$ mice, 1.0 ± 0.04. Peak currents were measured immediately following break through and were compared with currents averaged for values between 25 and 30 min. (**C**) NVP-AAM077 ($N=6$), but not Ro25-6981 ($N=5$), inhibits the potentiation of I_{NMDA} by PACAP38. The application of PACAP38 is indicated by the shaded region and was 5 min. (**D**) NVP-AAM077 ($N=6$) and Zn^{2+} ($N=6$), but not Ro25-6981 ($N=5$) or ifenprodil ($N=6$), prevents the enhancement of I_{NMDA} by PACAP38. Furthermore, PACAP38 cannot potentiate I_{NMDA} in GluN2A$^{-/-}$ mice ($N=5$) even though wild-type cells ($N=5$) demonstrated a degree of potentiation similar to that observed in rat neurons (1.4 ± 0.1 times control). Test reagents (PACAP38, 1 nM; NVP-AAM077, 50 nM; Ro25-6981, 500 nM; ifenprodil 3 μM; Zn^{2+}, 300 nM) were co-applied with NMDA/Glycine solutions using the multi-barreled perfusion system and were included in the bath during the entire recording period (not PACAP38). Peak currents were averaged for 5 min prior to applying PACAP and were compared with currents averaged for values between 20 and 25 min. **Indicates $P<0.01$, one-way ANOVA (Tukey's *post hoc* comparison). Calibration bars: 2 s; (**A**) Src 150 pA, Ro25-6981 200 pA; (**B**) PACAP38 200 pA, Ro25-6981 200 pA, NVP-AAM077 300 pA.

Importantly, increased GluN2A phosphorylation was prevented by applications of TAT-Src(40–58) (Figure 3B). Conversely, treatment of slices with SKF81297 (10 μM for 10 min) increased Fyn kinase activity, but not that of Src (Figure 3C), and increased tyrosine phosphorylation of GluN2B, but not GluN2A subunits (Figure 3D). The SKF81297-induced increase in GluN2B phosphorylation was prevented by a TAT-Fyn(39–57) (Figure 3D) as well as by a D1R antagonist (SCH23390, 10 μM).

Selectivity of GPCR activation upon NMDAR-mediated EPSCs in rat hippocampal slices

Bath application of PACAP38 (10 nM) or SKF81297 (20 μM) increased the amplitude of NMDAR-mediated EPSCs ($NMDAR_{EPSC}$) recorded from rat hippocampal slices (PACAP38: 1.59 ± 0.15, $n=5$; SKF81297: 1.78 ± 0.23, $n=6$) (Figure 4A and B). The effects of PACAP38 on $NMDAR_{EPSCs}$, previously shown to be prevented by Src(40–58) (Macdonald *et al*, 2005), were not affected by pipette applications of Fyn(39–57) (25 ng/ml, patch pipette) (Figure 4A). Conversely, the effect of SKF81297 was prevented by the Fyn(39–57), but not by the pipette applications of Src(40–58) (Figure 4B and C). We also recorded in the continued presence of bath applied Ro 25-6981 (500 nM), to block GluN2BRs, and demonstrated that $NMDAR_{EPSCs}$ were still potentiated when PACAP38 (Figure 4A) was applied. In contrast, the potentiation by SKF81297 (Figure 4B and C) was blocked by Ro 25-6981 (500 nM) and by the D1,5 antagonist, SCH 23390 (10 μM). Therefore, PACAP38 preferentially augments the function of synaptic GluN2ARs, but not GluN2BRs, by enhancing Src activity but not Fyn; and, SKF81297 selectively augments the function of synaptic GluN2BRs, but not GluN2ARs, by enhancing Fyn, but not Src, kinase activity.

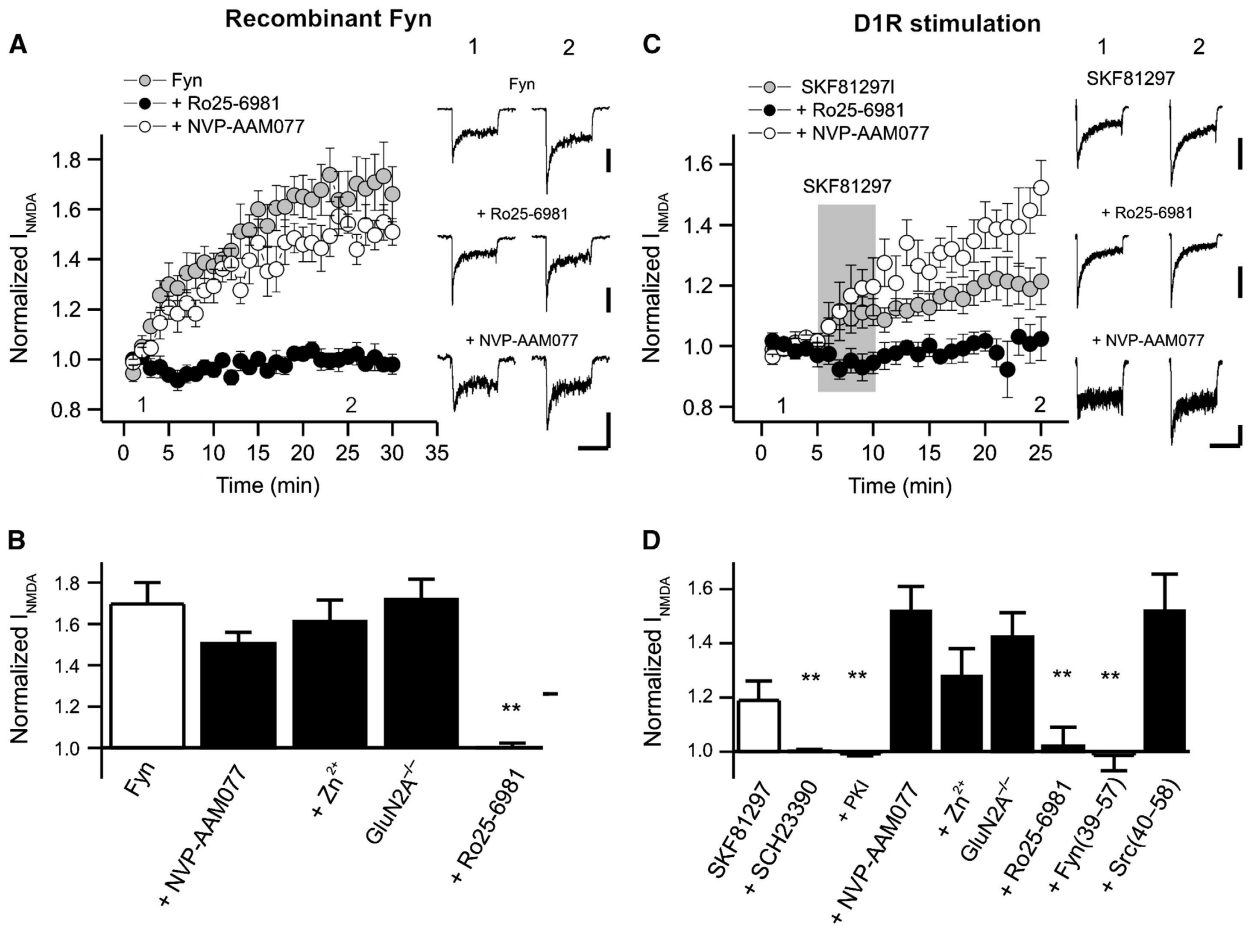

Figure 2 D1R-Fyn activation potentiates GluN2B-containing NMDAR currents in acutely isolated CA1 neurons of the rat and also in cells isolated from GluN2A$^{-/-}$ mice. (**A**) Fyn-dependent upregulation of I_{NMDA} ($N=6$) was blocked by Ro25-6981 ($N=6$) but not by NVP-AAM077 ($N=6$). (**B**) Quantification of normalized I_{NMDA} recorded from hippocampal neurons. Fyn potentiation of I_{NMDA} ($N=6$) is blocked by Ro25-6981 ($N=6$) but not by NVP-AAM077 ($N=6$) or Zn^{2+} ($N=7$). In cells taken from GluN2A$^{-/-}$ mice ($N=5$) Fyn enhanced NMDAR peak currents. Recombinant Fyn (1 U/ml) was applied via the patch pipette. NVP-AAM077, Zn^{2+}, and Ro25-6981 were applied to the bath and to the perfusion solutions containing NMDA/Glycine. Peak currents were measured immediately following break through and were compared with currents averaged for values between 25 and 30 min. (**C**) Upregulation of I_{NMDA} by SKF81297 ($N=9$) was blocked by Ro25-6981 ($N=7$) but not by NVP-AAM077 ($N=5$). The application of SKF81297 is indicated by the shaded region and was 5 min. (**D**) Quantification of normalized I_{NMDA} recorded from isolated hippocampal neurons treated with SKF81297. D1R-induced potentiation of I_{NMDA} ($N=9$) is prevented by SCH23390 ($N=9$), PKI_{5-24} ($N=7$), Ro25-6981 ($N=7$), and Fyn(39–57) ($N=5$) but not by NVP-AAM077 ($N=5$), Zn^{2+} ($N=8$), or Src(40-58) ($N=8$). In cells from GluN2A$^{-/-}$ mice, currents were enhanced by applications of SCH23390 ($N=6$). Test reagents (SKF81297, 10 μM; SCH23390, 10 μM; Ro25-6981 500 nM; Zn^{2+}, 300 nM; NVP-AAM077, 50 nM) were co-applied with NMDA/Glycine solutions using the multi-barreled perfusion system and were included in the bath when appropriate (not SKF81297). Fyn(39–57), 25 ng/ml; Src(40–58), 25 ng/ml and PKI_{5-24}, 300 nM were included in the patch pipettes. Peak currents were averaged for 5 min prior to applying SKF81297 and were compared with currents averaged for values between 20 and 25 min. **Indicates $P<0.01$, one-way ANOVA. Calibration bars: 2 s; (**A**) Fyn 150 pA, Ro25-6981 200 pA, NVP-AAM077 150 pA; (**B**) Control 400 pA, Ro25-6981 400 pA, NVP-AAM077 100 pA.

Selectivity of GPCR activation upon synaptic plasticity in hippocampal slices

We then examined the consequences of enhancing each receptor subtype on synaptic plasticity in rat hippocampal slices. Field excitatory postsynaptic potentials (fEPSPs) were recorded from the CA1 stratum radiatum in response to electrical stimulation of Schaffer-collaterals in rat hippocampal slices. In control slices, baseline was monitored for a minimum of 20 min before the induction of synaptic plasticity. In drug treated slices, baseline responses were monitored for 10 min before applying either PACAP38 (1 nM) or SKF81297 (10 μM) to the bath for 10 min (shaded regions in Figure 5) and was continued until just after the induction of synaptic plasticity. fEPSP slopes were unaffected by the bath application of either PACAP38 or SKF81297 (Supplementary Figure S3A). In addition, a separate series of recordings confirmed that neither treatment altered paired-pulse facilitation (Supplementary Figure S3B), a form of short-term plasticity used to assess changes in presynaptic function.

Changes in plasticity were characterized by varying the frequency of repetitive stimulation (1–100 Hz) used during the induction phase, thus generating frequency–plasticity relationship for each of our treatment conditions. In this way, we could monitor not only the maximum synaptic gain change but also the frequency at which the direction of plasticity changed from LTD to LTP. In control slices, maximum potentiation and depression were achieved following repetitive stimulation at 50 and 1 Hz, respectively; and the direction of plasticity changed from LTD to LTP at induction frequencies ranging from 10 to 20 Hz (Figure 5). Although

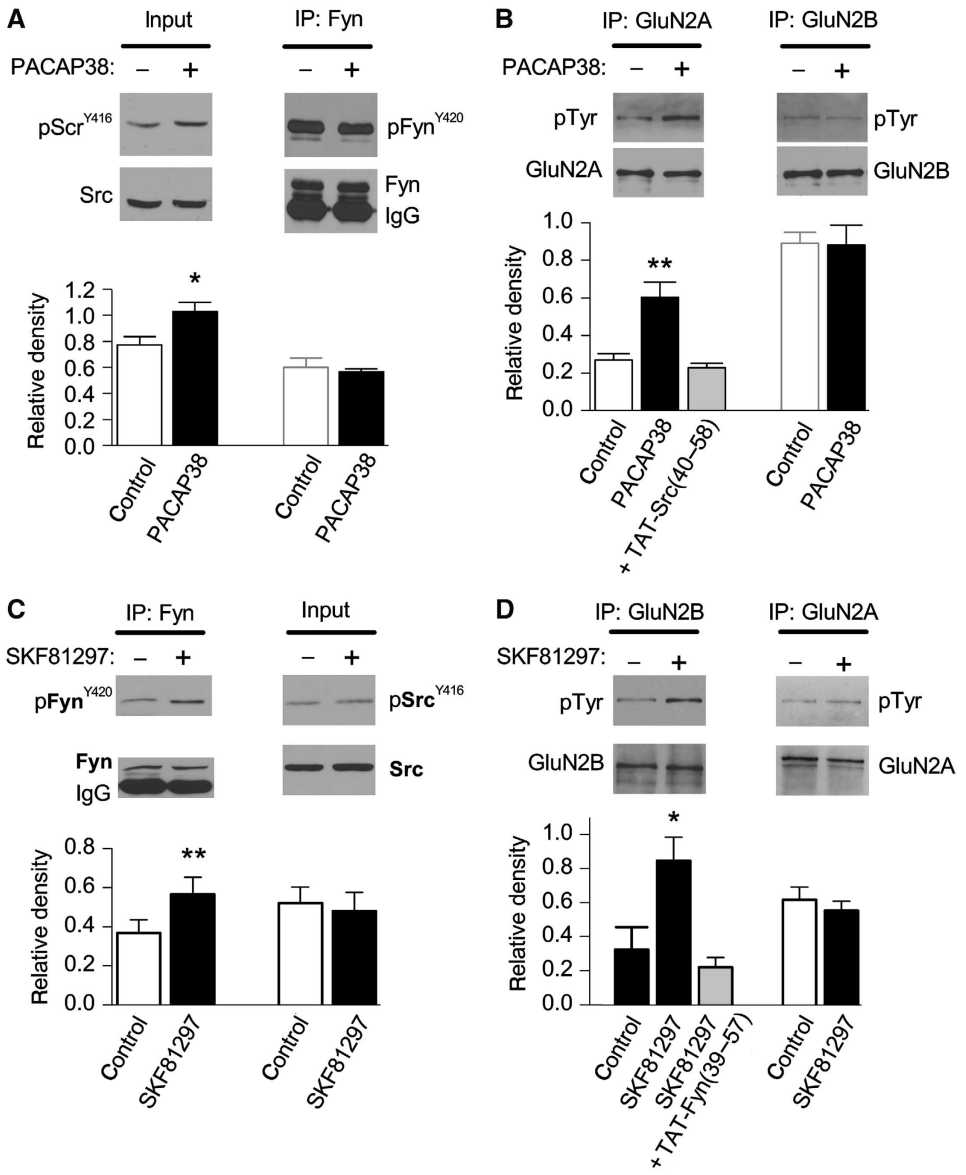

Figure 3 PACAP38 and SKF81297 activate Src and Fyn leading to phosphorylation of GluN2A and GluN2B. (**A**) PACAP38 (1 nM) treatment increases the phosphorylation of Src (pSrc^{Y416}) but not Fyn (pFyn^{Y420}). Below, summary of immunoblot analysis shows the averaged relative density of pSrc^{Y416} or pFyn^{Y420} for each condition ($n=4$). (**B**) PACAP38 treatment increases the tyrosine phosphorylation of immunoprecipitated GluN2A- but not GluN2B-containing NMDARs. The enhancement by PACAP38 was blocked by co-applications of TAT-Src(40–58). Below, the relative density of pTyr for GluN2A and GluN2B was quantified from immunoblots ($n=4$) for each of the conditions shown. (**C**) SKF81297 increases the phosphorylation of Fyn (pFyn^{Y420}) but not Src (pSrc^{Y416}). Below, the averaged relative density of pSrc^{y416} ($n=3$) or pFyn^{Y420} ($n=4$) from immunoblots obtained for each condition is shown (*below*). (**D**) SKF81297 (10 μM) treatment increases the tyrosine phosphorylation of immunoprecipitated GluN2B- but not GluN2A-containing NMDARs. The enhancement by SKF81297 was blocked by co-applications of TAT-Fyn(39–57). The averaged relative density of pTyr for GluN2A ($n=8$) and GluN2B ($n=3$) from immunoblots obtained under each of the conditions is shown. *Indicates $P<0.05$, *t*-test, **indicates $P<0.01$, Student's *t*-test. Figure source data can be found in Supplementary data.

LTD was consistently observed in control slices with 5–10 Hz stimulation, LTP was now observed at lower frequencies (Figure 5C; PACAP38 group at 10 and 20 Hz).

In contrast, the D1R agonist SKF81297 shifted the modification threshold to the right thereby increasing the threshold for LTP induction. As a result, LTD induction was now favoured (Figure 5; SKF81297 group at 1, 10, 20, and 50 Hz).

Although implied, our results do not definitively show that it is the phosphorylation of NMDARs that is responsible for the changes in the direction of the induction of synaptic plasticity. Indeed, other targets of these signalling cascades could also contribute to the changes in plasticity described. For this reason, we employed knock-in transgenic mice where key tyrosine residues were changed to phenylalanines (Nakazawa *et al*, 2006; Taniguchi *et al*, 2009; Delawary *et al*, 2010; Matsumura *et al*, 2010; Katano *et al*, 2011). Src enhancement of NMDAR-evoked currents is lost in GluN2A(Y1325F) mice (Taniguchi *et al*, 2009) and we determined if PACAP would potentiate NMDAR currents in isolated neurons taken from these mice. In parallel, we examined responses to SKF81297 in cells isolated from GluN2B(Y1472F) mice. PACAP38 and SKF81297 failed to potentiate NMDAR-induced currents in cells from GluN2A(Y1325F) and GluN2B(Y1472F) mice, respectively, even though the enhancements were observed in cells from wild-type mice (Figure 6A and B). Furthermore, PACAP38

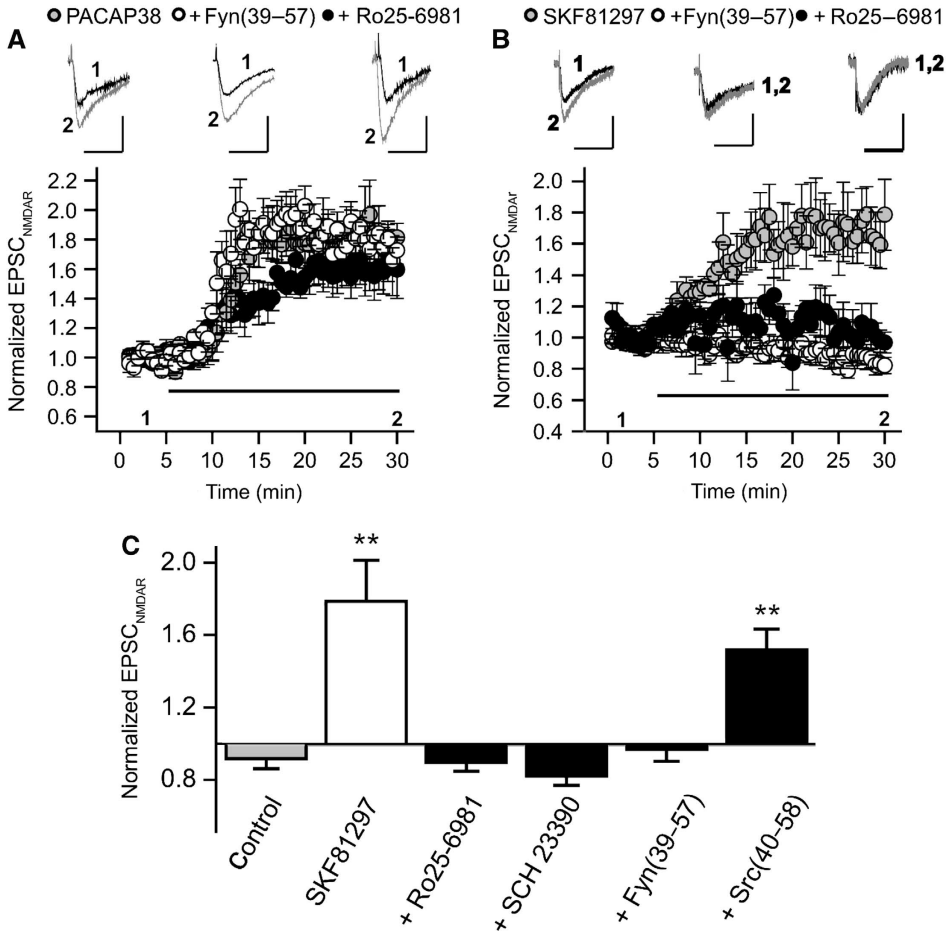

Figure 4 PACAP38 and SKF81297 increase GluN2AR- and GluN2BR-mediated synaptic currents via Src and Fyn, respectively. (**A**) The increase of $NMDAR_{EPSCs}$ by PACAP38 (5 nM; bath applied) ($N=8$) is unaffected by Ro25-6981 (500 nM; bath applied) ($N=6$) or by Fyn(39–57) (25 ng/ml, patch pipette) ($N=5$). (**B**) The increase of $NMDAR_{EPSCs}$ by SKF81297 (20 μM; bath applied) ($N=6$) is blocked by Ro25-6981 (500 nM; bath applied) ($N=6$) and by Fyn(39–57) (25 ng/ml patch pipette) ($N=4$). (**C**) The potentiation of $NMDAR_{EPSCs}$ by SKF81297 ($N=6$) could be prevented by SCH23390 (10 μM; bath applied) ($N=6$), Ro25-6981 (500 nM; bath applied) ($N=6$), Fyn(39–57) (25 ng/ml patch pipette) ($N=6$) but not by Src(40–58) (25 ng/ml patch pipette) ($N=6$). Peak currents were averaged for 5 min prior to applying PACAP and were compared with currents averaged for values between 25 and 30 min. **Indicates $P<0.01$, Student's *t*-test Calibration bars: 100 ms; (**A**) PACAP38 100 pA, Fyn(39–57) 100 pA, Ro25-6981 100 pA; (**B**) SKF81297 50 pA, Fyn(39–57) 35 pA, Ro25-6981 25 pA.

(1 nM) increased NMDAR-mediated currents in isolated neurons from GluN2B(Y1472F) ($n=5$ cells, 1.4 ± 0.14) mice and SKF81297 (10 μM) increased those taken from GluN2A (Y1325F) ($n=4$, 1.2 ± 0.02).

In order to establish that the changes in the direction of plasticity were directly dependent upon phosphorylation of GluN2AR and GluN2BRs, we examined slices from knock-in mice. We used a 10-Hz stimulus frequency, the frequency at which we observed a shift to LTP following application of PACAP (Figure 6C); or, alternatively a shift in favour of LTD following SKF81297 in slices from wild-type mice. Neither shift was observed in slices from GluN2A(Y1325F) and GluN2B(Y1472F) mice, respectively (Figure 6D and E). Importantly, we also observed no changes in the expression or activation of Src and Fyn in the hippocampus of these knock-in mice (Supplementary Figures S4 and S5).

Discussion

It is acknowledged that GluN2ARs and GluN2BRs can potentially provide very different temporal and spatial Ca^{2+} signals following synaptic stimulation. The magnitude and kinetics of these Ca^{2+} signals will also depend strongly upon the properties of the presynaptic afferent stimulation. The contributions of each subtype of NMDAR to postsynaptic plasticity will therefore change with the use of differing stimulus protocols. The data presented show that both Gαq- and Gαs-associated GPCRs enhance synaptic currents generated by NMDARs at CA1 synapses. However, they do so by respectively activating Src or Fyn, and, by selectively enhancing the contribution of GluN2AR versus GluN2BR to synaptic transmission. The Src-dependent enhancement of GluN2AR function facilitated LTP induction while LTD was facilitated when Fyn kinase, recruited through GPCR-initiated signalling cascades, enhanced GluN2BR function. It is important to note that what we have shown is that under our given set of stimulus protocols GluN2ARs and GluN2BRs can have very different effects on the direction of synaptic plasticity, presumably because they induce very different intracellular Ca^{2+} signals. Importantly, our findings are also consistent with biochemical and structural evidence (Kim *et al*, 2005; Shinohara *et al*, 2008), suggesting that GluN2BRs

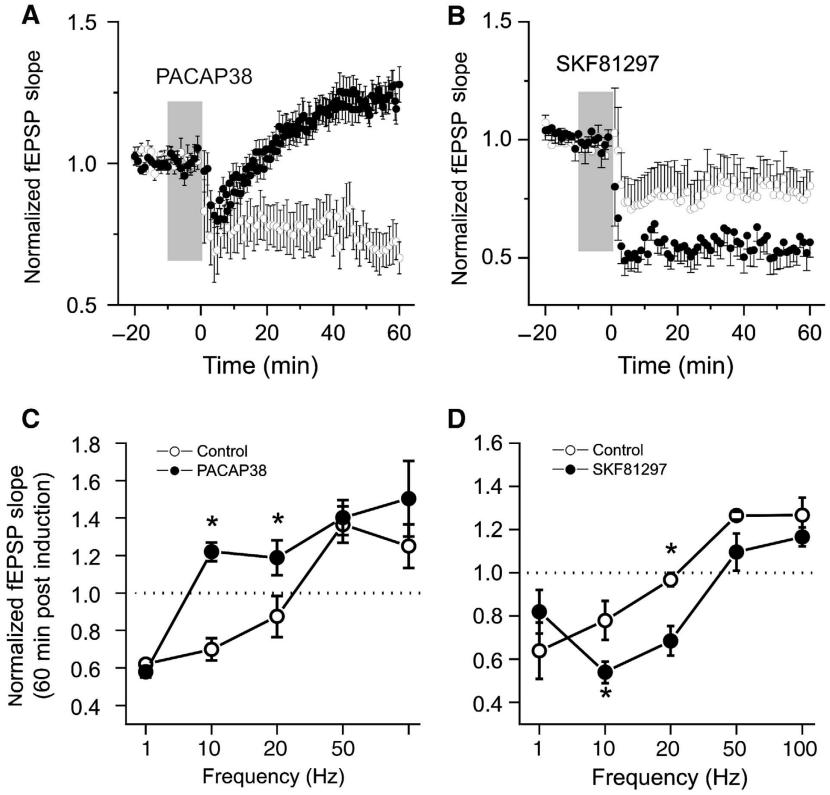

Figure 5 In rat hippocampal slices, PACAP38 application lowers the threshold for the induction of LTP whereas SKF81297 enhances LTD at stimulus frequencies near the threshold for the induction of LTP. (**A**) Control ($N=9$) and PACAP38-treated ($N=11$) slices (1 nM; bath applied for time indicated by shaded region) are shown. At time zero, the 10-Hz stimulation was performed. Post induction fEPSP slopes from each treatment group were normalized to baseline responses. (**B**) Control ($N=9$) and SKF81297-treated ($N=9$) slices (10 μM; 10 min bath applied for time indicated by shaded region) are shown. At time zero, the 10-Hz stimulation was performed. Post induction fEPSP slopes were normalized to baseline responses. (**C**) For a series of recordings from control or PACAP38 (1 nM, 10 min bath applied as indicated above) treated slices, fEPSP slopes were normalized to the mean slope measured during a 20-min baseline recording period. At $t=0$, repetitive stimulation, consisting of 600 pulses, was delivered at frequencies of 1, 10, 20, 50, or 100 Hz. Controls ($N=5$–11) and PACAP38 ($N=5$–9). The relative degree of potentiation or depression at the end of the recordings was plotted versus the stimulation frequency (1–100 Hz) used during the induction of plasticity. (**D**) As in (**C**) but for applications of control or SKF81297 (10 μM, 10 min bath applied) treated slices. Controls ($N=5$–9) and SKF81297 ($N=5$–9). The relative degree of potentiation or depression at the end of the recordings was plotted versus the stimulation frequency (1–100 Hz) used during the induction of plasticity. The average of slope measurements recorded over the last 10-min period (50–60 min) was employed in each case. *Indicates $P<0.001$, Student's *t*-test.

may promote AMPAR internalization, and, conversely that GluN2ARs may drive GluR1 delivery to synapses, a critical step for the induction of LTP (Shi *et al*, 2001). These studies thus provide a mechanistic basis for functional GluN2 subunit segregation with respect to the induction of bidirectional plasticity. Nevertheless, as both receptor subtypes contribute intracellular Ca^{2+} signals their effects on the direction of synaptic plasticity are likely to be dependent upon both temporal (e.g., kinetics of receptor activation) and topographical aspects (e.g., spine versus extra-spine locations) of each receptor subtype (Kohr, 2006). Just because, under our conditions, one signalling pathway favours LTP and the other LTD does not imply that this will be so under other conditions of stimulation. Rather our results demonstrate that these signalling pathways have the capacity to differentially regulate the direction of synaptic plasticity. For example, applications of D1R agonist have been reported to either enhance LTD (Liu *et al*, 2009) or alternatively enhance LTP via GluN2B and tyrosine kinases (Stramiello and Wagner, 2008).

A potential complication with our interpretations would be the existence of triheteromeric receptors (consisting of both GluN2A and GluN2B receptors) at CA1 synapses. There is little direct evidence for such GluN2ABRs, although there is accumulating indirect evidence based on the kinetics of NMDAR-mediated EPSCs (Grey *et al*, 2011; Rauner and Kohr, 2011), and the existence of such receptors has been proposed on the basis of functional and biochemical evidence (Hatton and Paoletti, 2005; Neyton and Paoletti, 2006; Paoletti and Neyton, 2007). Triheteromeric receptors demonstrate a pharmacological profile for the subunit selective antagonists, which is intermediate compared with diheteromeric receptors, albeit with less potency (Hatton and Paoletti, 2005; Neyton and Paoletti, 2006; Paoletti and Neyton, 2007). In our experiments, triheteromeric receptors would have been inhibited by blockers of both GluN2ARs and GluN2BRs, suggesting that either such receptors represent a relatively small proportion of the population in CA1 neurons or they show little selectivity for regulation by Src and Fyn kinases. This interpretation is supported by our demonstration of the insensitivity of NMDAR currents to Src but not Fyn kinase in CA1 neurons from GluN2A knockout mice.

Although conceptually elegant, the proposal that the direction of synaptic plasticity is determined by the subtype of NMDAR (Liu *et al*, 2004) has proven highly controversial

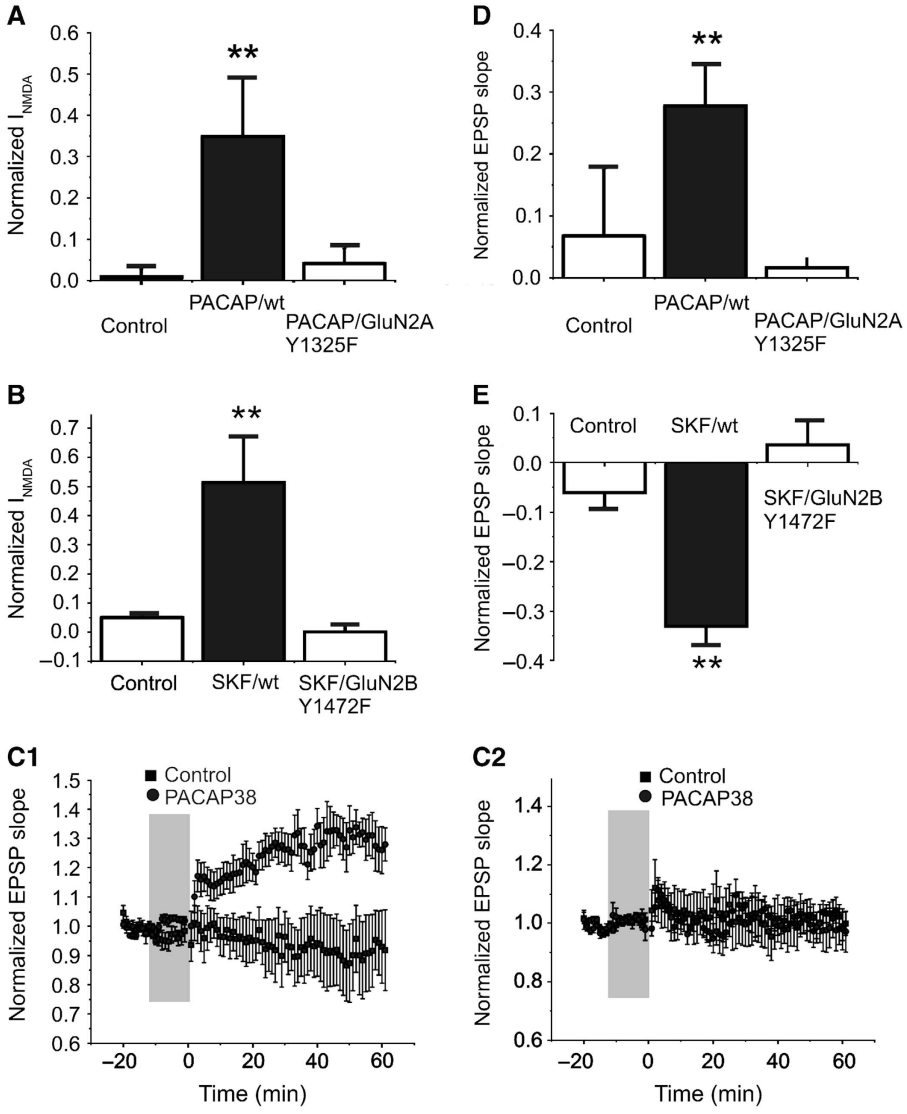

Figure 6 Enhancements of NMDA-evoked currents are lost in isolated cells from knock-in mice; and, so are the shifts in synaptic plasticity in mouse hippocampal slices. (**A**) The application of PACAP (1 nM, applied by multi-barreled perfusion) increased NMDA-evoked currents in acutely isolated CA1 hippocampal neurons from wild-type mice ($N=6$). In isolated neurons from GluN2A(Y1325F) knock-in mice, PACAP failed to increase NMDAR currents ($N=6$). (**B**) The treatment of isolated neurons, from wild-type mice, with SKF81297 ($N=5$) (10 min, 10 μM applied by multi-barreled perfusion) enhanced NMDAR currents. In contrast, the ability of SKF81297 to modulate NMDAR-mediated currents was lost in isolated cells from GluN2B(Y1472F) transgenic mice ($N=6$). (**C**) Responses of slices from wild-type (**C1**) and from GluN2A(Y1325F) knock-in mice (**C2**) are compared with and without applications of PACAP38 (1 nM, 10 min bath applied). The stimulus protocol was 600 pulses at 10 Hz applied at time zero. In controls ($N=6$), little or no LTP was observed but following PACAP38, a robust potentiation was observed ($N=6$). This facilitation of LTP induction by PACAP38 was absent in slices from the GluN2B(Y1325F) knock-in mice ($N=6$). (**D**) The effects of PACAP38 on plasticity are plotted. (**E**) The application of D1R agonist SKF81297 (10 min, bath applied, 10 μM) induced LTD in slices from wild-type mice ($N=5$), but this effect was lost in slices from GluN2B(Y1472F) knock-in mice ($N=6$). **Indicates $P<0.01$, Student's *t*-test.

with support, both for a unique role of GluN2BRs in the induction of LTD (versus GluN2ARs in LTP) (Liu *et al*, 2004; Fox *et al*, 2006; Howland and Wang, 2008; Gao *et al*, 2009; Brigman *et al*, 2010; Ge *et al*, 2010), and against such a proposed model (see Berberich *et al*, 2005 and Morishita *et al*, 2007). The controversy may in part originate from limitations inherent in the tools used to distinguish between these receptors as well as from differences in methodologies. For example, NVP-AAM077 has a limited ability to distinguish between these receptor subtypes (~10-fold). Equally important, as NVP-AAM077 is a competitive antagonist, its effectiveness is determined by the concentration of released glutamate, which co-varies with the stimulation frequency used during plasticity induction. Methodological differences that impact transmitter release probability and re-uptake will therefore influence the effectiveness of NVP-AAM077. Further, GluN2BRs and GluN2ARs have differing affinities for glutamate and their respective contribution to the total NMDAR-mediated Ca^{2+} signals generated during the vastly different protocols used to elicit LTP/LTD will differ substantially (Hatton and Paoletti, 2005; Neyton and Paoletti, 2006; Paoletti and Neyton, 2007). The interpretation of slice experiments conducted in the presence of NVP-AAM077 is therefore problematic. Genetic approaches (e.g., deletion or overexpression of a protein of interest) also have their limitations as they may distort the normal interplay between protein

complexes expressed at the postsynaptic density (e.g., developmental compensation for the genetic deletion of a Src family kinase or GluN2 subunit). Another factor is that studies examining changes in the GluN2A to GluN2B subunit ratio have not distinguished relative changes from absolute changes in one or the other subtype of receptor (Cho *et al*, 2009) nor do they necessarily distinguish acute changes in receptor activity from changes in expression. For example, an increase in the ratio could originate as a consequence of decreasing GluN2BRs or alternatively by increasing GluN2ARs without a corresponding change in the function of the other subtype. Whereas the outcome of the former is a net loss of synaptic NMDAR currents, the latter generates a net gain. The direction of plasticity change is likely determined, not only by the ratio of each sub-population of receptors, but also by the absolute level of synaptic NMDAR activation achieved. Consequently, how NMDAR subunit ratio changes are achieved may be a cardinal distinguishing feature underlying various forms of metaplasticity.

Our findings show that GPCRs can determine the direction of synaptic plasticity by dynamically determining the contributions of GluN2ARs and GluN2BRs. This is achieved via distinct signalling cascades, each of which targets respective receptor subtypes by means of the Src family kinases, Src and Fyn. Src family cascades effectively enhance NMDAR responses at hippocampal synapses (Yaka *et al*, 2003; Macdonald *et al*, 2005) as well as at prefrontal cortical synapses (Salter and Kalia, 2004; Lei *et al*, 2009) but the consequences on synaptic plasticity can be dramatically different. Therefore, their capacity to regulate learning and memory is also likely to be substantially more complex. This complexity is likely to be of substantial relevance to the efforts that are being made to treat the negative cognitive symptoms of schizophrenia by pharmacologically enhancing NMDAR responses (Kantrowitz and Javitt, 2010; Kantrowitz *et al*, 2010). Indeed, deficits in the expression of GluN2B have been implicated in schizophrenia and include potential polymorphisms in *Grin2B* (gene for GluN2B) as well as selective reductions in expression of GluN2B (Bjarnadottir *et al*, 2007; Kristiansen *et al*, 2007, 2010; Campo *et al*, 2009; Kochlamazashvili *et al*, 2010). Our results strongly imply that attempts to enhance NMDAR function must also aim to restore the appropriate balance between GluN2A and GluN2B receptors in order to mitigate negative symptoms of schizophrenia.

Materials and methods

Cell isolation and whole-cell recordings

CA1 neurons were isolated from postnatal rats (Wistar, 14–22 days) or postnatal mice (28–34 days) using previously described procedures (Wang and MacDonald, 1995). To control for variation in response, recordings from control and treated cells were made on the same day. The extracellular solution consisted of the following (in mM): 140 NaCl, 1.3 $CaCl_2$, 5 KCl, 25 HEPES, 33 glucose, and 0.0005 tetrodotoxin, pH 7.4 (osmolality between 315 and 325 mOsm). Recording electrodes with resistances of 3–5 MΩ were constructed from borosilicate glass (1.5 μm diameter; World Precision Instruments, Sarasota, FL) using a two-stage puller (PP83; Narishige, Tokyo, Japan) and filled with intracellular solution containing the following (in mM): 140 CsF, 11 EGTA, 1 $CaCl_2$, 2 $MgCl_2$, 10 HEPES, 2 tetraethylammonium, and $2K_2ATP$, pH 7.2 (osmolality between 290 and 300 mOsm). Where indicated, some drugs were included in the patch pipette. Recordings were conducted at room temperature (20–22°C). After formation of the whole-cell configuration, the neurons were voltage clamped at −60 mV and lifted into the stream of solution supplied by a computer-controlled, multi-barreled perfusion system (SF-77 B, Warner Instrument Corporation). The exchange time for solutions was ∼30–50 ms. To monitor access resistance, a voltage step of −10 mV was made before each application of NMDA. When series resistance increased to >20 MΩ, the cell was discarded. Currents were recorded using an Axopatch 1D amplifier. Data were filtered at 2 kHz and digitized at 10 kHz using Clampex software. All population data are expressed as mean ± s.e. Student's *t*-test was used to compare between two groups and the one-way ANOVA test (*Tukey's post hoc comparison)* was used to analyse multiple groups.

Zn^{2+}-buffered solutions

The tricine-buffered zinc solutions were prepared according to the empirically established binding constant by adding into 10 mM tricine and as previously described (Nozaki *et al*, 2011). The amount of $ZnCl_2$ required can be calculated based on the following formula: $[Zn]_{free} = [ZnCl_2]_{total}/300$. (At pH 7.3; with 10 mM tricine for $[Zn]_{free} = 300$ nM.)

Preparation of rat and mouse hippocampal slices

Wistar rats (3–4-week old) or transgenic mice (4–6-week old) were anaesthetized using isoflurane and immediately decapitated. The brains were rapidly removed and submerged in chilled (4°C) oxygenated (95% O_2/5% CO_2) artificial cerebrospinal fluid (aCSF) composed of (in mM): NaCl (124), KCl (3), $CaCl_2$ (2.6), $MgCl_2$ (1.3), $NaHCO_3$ (26), NaH_2PO_4 (1.25) and D-glucose (10) with osmolality adjusted to 300–310 mOsM and pH to 7.4. Transverse hippocampal slices (350 μm) were cut using a vibrotome (VT1000E; Leica). Slices were allowed to recover in a submerged holding chamber for 60–90 min under continuous oxygenation until needed. For recording, a single slice was transferred to a recording chamber, immobilized with a platinum wire grid and continuously superfused with oxygenated aCSF.

Recording of fEPSPs

fEPSPs were evoked at a frequency of 0.05 Hz by electrical stimulation (100 μs duration) delivered to the Schaffer-collateral pathway using a concentric bipolar stimulating electrode (25 μm exposed tip), and recorded using glass microelectrodes (3–5 MΩ filled with aCSF) positioned in the stratum radiatum layer of the CA1 subfield. Peak amplitudes and slopes were recorded and measured. Electrode depth was varied until a maximal response was elicited (∼175 μm from surface). The input–output relationship was first determined in each slice by varying stimulus intensity (10–1000 μA) and recording the corresponding fEPSP. Using a stimulus intensity that evoked 30–40% of the maximal fEPSP, paired-pulse responses were measured every 20 s by delivering two stimuli in rapid succession with intervals (interstimulus interval, ISI) varying from 10 to 1000 ms. Following this protocol, fEPSPs were evoked and measured for 20 min at 0.05 Hz using the same stimulus intensity to test for stability of the response. At this time, plasticity was induced by 1, 10, 20, 50, or 100 Hz stimulation with train pulse number constant at 600. Any treatments were added to aCSF and applied to the slice for the 10 min immediately prior to the induction of plasticity.

Whole-cell recordings from rat hippocampal slices

Tight-seal whole-cell recordings from CA1 pyramidal neurons were obtained using either a visually guided or blind-patch approach. Patch pipettes (4–6 MΩ) were filled with internal solution containing (in mM): Cs-gluconate 132.5, CsCl 17.5, HEPES 10, EGTA 0.2, Mg-ATP 2, and GTP 0.3 (pH 7.25, 290 mOsm). To pharmacologically isolate NMDAR-mediated EPSCs, bicuculline (10 μM) and CNQX (10 μM) were added to the ACSF. In neurons voltage clamped at −60 mV, synaptic responses were evoked with a concentric bipolar tungsten electrode located about 50 μm from the cell body layer in CA1. Test stimuli were evoked at 0.05 Hz with the stimulus intensity set to 25–50% of the maximal synaptic response. PACAP (10 nM) or SKF81297 (20 μM) was applied after 5 min of a stable baseline period, and NMDAR EPSCs were recorded for the subsequent 20–25 min. In some experiments, slices were pretreated with Ro 25-6981 (0.5 μM) or SCH23390 (10 μM). In others, Fyn inhibitor peptide (25 μg/ml) or Src(40–58) inhibitor peptide (25 μg/ml) were added to the pipette solution. Data were used only after the access resistance had stabilized. Series resistance ranged from 10 to 20 MΩ,

as estimated from series resistance compensation of current responses to voltage steps of 5 mV. Signals were recorded using a Multiclamp 700A, sampled at 10 kHz, and analysed with Clampfit 9.2 software.

Immunoprecipitation and western blotting

Hippocampal slices were prepared from Wistar rats (PN 15–20) or wild-type and transgenic mice (4–6-week old) and incubated in aCSF saturated with 95% O_2 and 5% CO_2 for at least 1 h at room temperature. This was followed by treatment with PACAP (1 nM for 15 min), SKF81297 (10 μM for 10 min), and their vehicles for control. For experiments testing Src(40–58), Fyn(39–57), or D1 receptor inhibition, the slices were pretreated with TAT-Src_{40-58} (10 μM), or TAT-Fyn_{ipep}, (10 μM), or SCH23390 (10 μM) 30 min before drug exposures. After three washes with cold PBS, slices were homogenized in ice-cold RIPA buffer (50 mM Tris–HCl pH 7.4, 150 mM NaCl, 1 mM EDTA, 0.1% SDS, 0.5% Triton X-100, and 1% Sodium Deoxycholate) supplemented with 1 mM sodium orthovanadate and 1% protease inhibitor cocktail, 1% protein phosphatases inhibitor cocktails, and subsequently spun at 16 000 r.c.f. for 30 min at 4°C (Eppendorf Centrifuge 5415R). The supernatant was collected and kept at −70°C. For immunoprecipitation, the sample containing 500 μg protein was incubated with antibodies (see below) at 4°C and gently shaken overnight. Antibodies used for immunoprecipitation were anti-NR2A and anti-NR2B (3 μg, rabbit IgG; Enzo Life Sciences, PA), anti-Src (1:500, mouse IgG; Cell Signaling Technology (CST), Danvers, MA), anti-Fyn (1:200, mouse IgG; Santa Cruz Biotechnology, Santa Cruz, CA). The immune complexes were collected with 20 μl of protein A/G–Sepharose beads for 2 h at 4°C. Immunoprecipitates were then washed three times with ice-cold PBS, resuspended in 2 × Laemmli sample buffer and boiled for 5 min. These samples were subjected to SDS–PAGE and transferred onto a nitrocellulose membrane. The blotting analysis was performed by repeated stripping and successive probing with antibodies: anti-pY(4G10) (1:2000, mouse IgG; Millipore Corp., Billerica, MA), GluN2A or GluN2B (1:1000, rabbit IgG; CST), $pSrc^{Y416}$ (1:1500, rabbit IgG; CST).

Drugs and peptides

The source of drugs for this study is as follows: Tricine, $ZnCl_2$, NMDA, glycine and R0 25-6981 (Sigma, St Louis, MO), Src ($p60^{c\text{-}Src}$) and Fyn (active) (Upstate Biotechnology), PACAP and VIP (Calbiochem, San Diego, CA). NVP-AAM077 was provided by Dr YP Auberson (Novartis Pharma AG, Basel, Switzerland). Src(40–58) and Scramble Src(40–58) were provided by Dr MW Salter (Hospital for sick children, Toronto, Ontario). Peptides were synthesized by the Advanced Protein Technology Centre (Toronto, Ontario, Canada) with the following sequences: Fyn(39–57) (YPSFGVTSIPNYNNFHAAG, Fyn amino acids 39–57), scrambled Fyn(39–57) (PSAYGNPGSAYFNFTNVHI). We attached both Src(40–58) and Fyn(39–57) to Tat transduction domains (YGRLLRQRRR), which allowed us to apply these membrane permeant forms of the selective Src versus Fyn interfering peptides extracellularly to hippocampal slices.

Transgenic mice

Heterozygous GluN2A(Y1325F) and GluN2B(Y1472F) were successively backcrossed to C57BL/6J mice to yield subsequent generations with a pure C57BL/6J genetic background. F10 heterozygous mice were crossed to each other to yield homozygous mice and wild-type littermates as previously described (Nakazawa *et al*, 2006). $GluN2A^{-/-}$ mice were generated from heterozygous matings (Kutsuwada *et al*, 1996). In experiments with GluN2A(1325F) mice, sodium orthovanadate (10 μM) was added to the bathing solutions.

Animal care

All animal experimentation was conducted in accordance with the Policies on the Use of Animals at the University of Toronto and the University of Western Ontario.

Supplementary data

Supplementary data are available at *The EMBO Journal* Online (http://www.embojournal.org).

Acknowledgements

This study was supported by a grant to JFM from CIHR. We thank Dr AM Craig for the $GluN2A^{-/-}$ mice and Dr YP Auberson for the gift of NVP-AAM077.

Author contributions: KY and CT designed and performed whole-cell voltage-clamp recordings from acutely isolated hippocampal neurons. BS and KY designed and performed extracellular field recordings from hippocampal slices. YFX and HL designed and performed whole-cell voltage-clamp recordings from CA1 pyramidal neurons in slice. GL designed and performed all immunoblotting. TN and TY provided GluN2A(Y1325F) and GluN2B(Y1472F) transgenic mice. MWS, BAO, and MFJ contributed to the design of experiments and co-supervised parts of the project. JFM conceptualized and supervised the project and contributed to the design of experiments. MFJ and JFM wrote the manuscript. All authors read and approved the final manuscript.

Conflict of interest

The authors declare that they have no conflict of interest.

References

Abraham WC (2008) Metaplasticity: tuning synapses and networks for plasticity. *Nat Rev Neurosci* **9:** 387

Ali DW, Salter MW (2001) NMDA receptor regulation by Src kinase signalling in excitatory synaptic transmission and plasticity. *Curr Opin Neurobiol* **11:** 336–342

Bartlett TE, Bannister NJ, Collett VJ, Dargan SL, Massey PV, Bortolotto ZA, Fitzjohn SM, Bashir ZI, Collingridge GL, Lodge D (2007) Differential roles of NR2A and NR2B-containing NMDA receptors in LTP and LTD in the CA1 region of two-week old rat hippocampus. *Neuropharmacology* **52:** 60–70

Berberich S, Jensen V, Hvalby O, Seeburg PH, Kohr G (2007) The role of NMDAR subtypes and charge transfer during hippocampal LTP induction. *Neuropharmacology* **52:** 77–86

Berberich S, Punnakkal P, Jensen V, Pawlak V, Seeburg PH, Hvalby O, Kohr G (2005) Lack of NMDA receptor subtype selectivity for hippocampal long-term potentiation. *J Neurosci* **25:** 6907–6910

Bjarnadottir M, Misner DL, Haverfield-Gross S, Bruun S, Helgason VG, Stefansson H, Sigmundsson A, Firth DR, Nielsen B, Stefansdottir R, Novak TJ, Stefansson K, Gurney ME, Andresson T (2007) Neuregulin1 (NRG1) signaling through Fyn modulates NMDA receptor phosphorylation: differential synaptic function in NRG1 +/− knock-outs compared with wild-type mice. *J Neurosci* **27:** 4519–4529

Brigman JL, Wright T, Talani G, Prasad-Mulcare S, Jinde S, Seabold GK, Mathur P, Davis MI, Bock R, Gustin RM, Colbran RJ, Alvarez VA, Nakazawa K, Delpire E, Lovinger DM, Holmes A (2010) Loss of GluN2B-containing NMDA receptors in CA1 hippocampus and cortex impairs long-term depression, reduces dendritic spine density, disrupts learning. *J Neurosci* **30:** 4590–4600

Campo CG, Sinagra M, Verrier D, Manzoni OJ, Chavis P (2009) Reelin secreted by GABAergic neurons regulates glutamate receptor homeostasis. *PLoS One* **4:** E5505

Cepeda C, Levine MS (2006) Where do you think you are going? The NMDA-D1 receptor trap. *Sci STKE* **2006:** E20

Chen BS, Roche KW (2007) Regulation of NMDA receptors by phosphorylation. *Neuropharmacology* **53:** 362–368

Cho KK, Khibnik L, Philpot BD, Bear MF (2009) The ratio of NR2A/B NMDA receptor subunits determines the qualities of ocular dominance plasticity in visual cortex. *Proc Natl Acad Sci USA* **106:** 5377–5382

Collingridge GL, Bliss TV (1995) Memories of NMDA receptors and LTP. *Trends Neurosci* **18:** 54–56

Cull-Candy SG, Leszkiewicz DN (2004) Role of distinct NMDA receptor subtypes at central synapses. *Sci STKE* **2004:** Re16

Delawary M, Tezuka T, Kiyama Y, Yokoyama K, Inoue T, Hattori S, Hashimoto R, Umemori H, Manabe T, Yamamoto T, Nakazawa T

(2010) NMDAR2B tyrosine phosphorylation regulates anxiety-like behavior and CRF expression in the amygdala. *Mol Brain* **3:** 37

Fischer G, Mutel V, Trube G, Malherbe P, Kew JN, Mohacsi E, Heitz MP, Kemp JA (1997) Ro 25-6981, a highly potent and selective blocker of N-methyl-D-aspartate receptors containing the NR2B subunit. Characterization *in vitro*. *J Pharmacol Exp Ther* **283:** 1285–1292

Fox CJ, Russell KI, Wang YT, Christie BR (2006) Contribution of NR2A and NR2B NMDA subunits to bidirectional synaptic plasticity in the hippocampus *in vivo*. *Hippocampus* **16:** 907–915

Gao LC, Wang YT, Lao X, Wang C, Wang FY, Yuan CG (2009) [The change of learning, memory ability in the rat model of depression]. *Fen Zi Xi Bao Sheng Wu Xue Bao* **42:** 20–26

Ge Y, Dong Z, Bagot RC, Howland JG, Phillips AG, Wong TP, Wang YT (2010) Hippocampal long-term depression is required for the consolidation of spatial memory. *Proc Natl Acad Sci USA* **107:** 16697–16702

Gingrich JR, Pelkey KA, Fam SR, Huang Y, Petralia RS, Wenthold RJ, Salter MW (2004) Unique domain anchoring of Src to synaptic NMDA receptors via the mitochondrial protein NADH dehydrogenase subunit 2. *Proc Natl Acad Sci USA* **101:** 6237–6242

Gray JA, Shi Y, Usui H, During J, Sakimura K, Nicoll RA (2011) Distinct modes of AMPA receptor suppression at developing synapses by GluN2A and GluN2B: single-cell NMDA receptor subunit deletion *in vivo*. *Neuron* **71:** 1085–1101

Hatton CJ, Paoletti P (2005) Modulation of triheteromeric NMDA receptors by N-terminal domain ligands. *Neuron* **46:** 261–274

Howland JG, Wang YT (2008) Synaptic plasticity in learning and memory: stress effects in the hippocampus. *Prog Brain Res* **169:** 145–158

Huang YQ, Lu WY, Ali DW, Pelkey KA, Pitcher GM, Lu YM, Aoto H, Roder JC, Sasaki T, Salter MW, MacDonald JF (2001) CAK beta/Pyk2 kinase is a signaling link for induction of long-term potentiation in CA1 hippocampus. *Neuron* **29:** 485–496

Ito I, Futai K, Katagiri H, Watanabe M, Sakimura K, Mishina M, Sugiyama H (1997) Synapse-selective impairment of NMDA receptor functions in mice lacking NMDA receptor epsilon 1 or epsilon 2 subunit [in process citation]. *J Physiol (Lond)* **500:** 401–408

Kantrowitz JT, Javitt DC (2010) N-methyl-D-aspartate (NMDA) receptor dysfunction or dysregulation: the final common pathway on the road to schizophrenia? *Brain Res Bull* **83:** 108–121

Kantrowitz JT, Malhotra AK, Cornblatt B, Silipo G, Balla A, Suckow RF, D'souza C, Saksa J, Woods SW, Javitt DC (2010) High dose D-serine in the treatment of schizophrenia. *Schizophr Res* **121:** 125–130

Katano T, Nakazawa T, Nakatsuka T, Watanabe M, Yamamoto T, Ito S (2011) Involvement of spinal phosphorylation cascade of Tyr1472-NR2B, Thr286-CaMKII, and Ser831-GluR1 in neuropathic pain. *Neuropharmacology* **60:** 609–616

Kim MJ, Dunah AW, Wang YT, Sheng M (2005) Differential roles of NR2A- and NR2B-containing NMDARs in Ras-ERK signaling and AMPA receptor trafficking. *Neuron* **46:** 745–760

Kochlamazashvili G, Senkov O, Grebenyuk S, Robinson C, Xiao MF, Stummeyer K, Gerardy-Schahn R, Engel AK, Feig L, Semyanov A, Suppiramaniam V, Schachner M, Dityatev A (2010) Neural cell adhesion molecule-associated polysialic acid regulates synaptic plasticity and learning by restraining the signaling through GluN2B-containing NMDA receptors. *J Neurosci* **30:** 4171–4183

Kohr G (2006) NMDA receptor function: subunit composition versus spatial distribution. *Cell Tissue Res* **326:** 439–446

Kristiansen LV, Huerta I, Beneyto M, Meador-Woodruff JH (2007) NMDA receptors and schizophrenia. *Curr Opin Pharmacol* **7:** 48–55

Kristiansen LV, Patel SA, Haroutunian V, Meador-Woodruff JH (2010) Expression of the NR2B-NMDA receptor subunit and its Tbr-1/CINAP regulatory proteins in postmortem brain suggest altered receptor processing in schizophrenia. *Synapse* **64:** 495–502

Kutsuwada T, Sakimura K, Manabe T, Takayama C, Katakura N, Kushiya E, Natsume R, Watanabe M, Inoue Y, Yagi T, Aizawa S, Arakawa M, Takahashi T, Nakamura Y, Mori H, Mishina M (1996) Impairment of suckling response, trigeminal neuronal pattern formation, and hippocampal LTD in NMDA receptor E2 subunit mutant mice. *Neuron* **16:** 333–344

Lei G, Anastasio NC, Fu Y, Neugebauer V, Johnson KM (2009) Activation of dopamine D1 receptors blocks phencyclidine-induced neurotoxicity by enhancing N-methyl-D-aspartate receptor-mediated synaptic strength. *J Neurochem* **109:** 1017–1030

Liu J, Wang F, Huang C, Long LH, Wu WN, Cai F, Wang JH, Ma LQ, Chen JG (2009) Activation of phosphatidylinositol-linked novel D1 dopamine receptor contributes to the calcium mobilization in cultured rat prefrontal cortical astrocytes. *Cell Mol Neurobiol* **29:** 317–328

Liu L, Wong TP, Pozza MF, Lingenhoehl K, Wang Y, Sheng M, Auberson YP, Wang YT (2004) Role of NMDA receptor subtypes in governing the direction of hippocampal synaptic plasticity. *Science* **304:** 1021–1024

Lu YM, Roder JC, Davidow J, Salter MW (1998) Src activation in the induction of long-term potentiation in CA1 hippocampal neurons. *Science* **279:** 1363–1367

Macdonald DS, Weerapura M, Beazely MA, Martin L, Czerwinski W, Roder JC, Orser BA, MacDonald JF (2005) Modulation of NMDA receptors by pituitary adenylate cyclase activating peptide in CA1 neurons requires Galphaq, protein kinase C, and activation of Src. *J Neurosci* **25:** 11374–11384

MacDonald JF, Jackson MF, Beazely MA (2007) G protein-coupled receptors control NMDARS and metaplasticity in the hippocampus. *Biochim Biophys Acta* **1768:** 941–951

Malherbe P, Mutel V, Broger C, Perin-Dureau F, Kemp JA, Neyton J, Paoletti P, Kew JN (2003) Identification of critical residues in the amino terminal domain of the human NR2B subunit involved in the Ro 25-6981 binding pocket. *J Pharmacol Exp Ther* **307:** 897–905

Matsumura S, Kunori S, Mabuchi T, Katano T, Nakazawa T, Abe T, Watanabe M, Yamamoto T, Okuda-Ashitaka E, Ito S (2010) Impairment of CaMKII activation and attenuation of neuropathic pain in mice lacking NR2B phosphorylated at Tyr1472. *Eur J Neurosci* **32:** 798–810

Morishita W, Lu W, Smith GB, Nicoll RA, Bear MF, Malenka RC (2007) Activation of NR2B-containing NMDA receptors is not required for NMDA receptor-dependent long-term depression. *Neuropharmacology* **52:** 71–76

Nakazawa T, Komai S, Watabe AM, Kiyama Y, Fukaya M, Rima-Yoshida F, Horai R, Sudo K, Ebine K, Delawary M, Goto J, Umemori H, Tezuka T, Iwakura Y, Watanabe M, Yamamoto T, Manabe T (2006) NR2B tyrosine phosphorylation modulates fear learning as well as amygdaloid synaptic plasticity. *Embo J* **25:** 2867–2877

Neyton J, Paoletti P (2006) Relating NMDA receptor function to receptor subunit composition: limitations of the pharmacological approach. *J Neurosci* **26:** 1331–1333

Nozaki C, Vergnano AM, Filliol D, Ouagazzal AM, Le GA, Carvalho S, Reiss D, Gaveriaux-Ruff C, Neyton J, Paoletti P, Kieffer BL (2011) Zinc alleviates pain through high-affinity binding to the NMDA receptor NR2A subunit. *Nat Neurosci* **14:** 1017–1022

Paoletti P, Neyton J (2007) NMDA receptor subunits: function and pharmacology. *Curr Opin Pharmacol* **7:** 39–47

Rauner C, Kohr G (2011) Triheteromeric NR1/NR2A/NR2B receptors constitute the major N-methyl-D-aspartate receptor population in adult hippocampal synapses. *J Biol Chem* **286:** 7558–7566

Salter MW, Kalia LV (2004) Src kinases: a hub for NMDA receptor regulation. *Nat Rev Neurosci* **5:** 317–328

Shi S, Hayashi Y, Esteban JA, Malinow R (2001) Subunit-specific rules governing AMPA receptor trafficking to synapses in hippocampal pyramidal neurons. *Cell* **105:** 331–343

Shinohara Y, Hirase H, Watanabe M, Itakura M, Takahashi M, Shigemoto R (2008) Left-right asymmetry of the hippocampal synapses with differential subunit allocation of glutamate receptors. *Proc Natl Acad Sci USA* **105:** 19498–19503

Stramiello M, Wagner JJ (2008) D1/5 receptor-mediated enhancement of LTP requires PKA, Src family kinases, and NR2B-containing NMDARS. *Neuropharmacology* **55:** 871–877

Taniguchi S, Nakazawa T, Tanimura A, Kiyama Y, Tezuka T, Watabe AM, Katayama N, Yokoyama K, Inoue T, Izumi-Nakaseko H, Kakuta S, Sudo K, Iwakura Y, Umemori H, Inoue T, Murphy NP, Hashimoto K, Kano M, Manabe T, Yamamoto T (2009) Involvement of NMDAR2A tyrosine phosphorylation in depression-related behaviour. *EMBO J* **28:** 3717–3729

Vicini S, Wang JF, Li JH, Zhu WJ, Wang YH, Luo JH, Wolfe BB, Grayson DR (1998) Functional and pharmacological differences between recombinant N-methyl-D-aspartate receptors. *J Neurophysiol* **79:** 555–566

Wang LY, MacDonald JF (1995) Modulation by magnesium of the affinity of NMDA receptors for glycine in murine hippocampal neurones. *J Physiol* **486** (Pt 1)**:** 83–95

Whitlock JR, Heynen AJ, Shuler MG, Bear MF (2006) Learning induces long-term potentiation in the hippocampus. *Science* **313:** 1093–1097

Xu J, Weerapura M, Ali MK, Jackson MF, Li H, Lei G, Xue S, Kwan CL, Manolson MF, Yang K, MacDonald JF, Yu XM (2008) Control of excitatory synaptic transmission by C-terminal Src kinase. *J Biol Chem* **283:** 17503–17514

Yaka R, He DY, Phamluong K, Ron D (2003) Pituitary adenylate cyclase-activating polypeptide (PACAP(1-38)) enhances N-methyl-D-aspartate receptor function and brain-derived neurotrophic factor expression via Rack1. *J Biol Chem* **278:** 9630–9638

Yang K, Trepanier CH, Li H, Beazely MA, Lerner EA, Jackson MF, MacDonald JF (2009) Vasoactive intestinal peptide acts via multiple signal pathways to regulate hippocampal NMDA receptors and synaptic transmission. *Hippocampus* **19** (9)**:** 779–789

